AN INTERCOMPARISON OF LARGE-EDDY SIMULATIONS OF THE STABLE BOUNDARY LAYER

ROBERT J. BEARE[1,*], MALCOLM K. MACVEAN[1], ALBERT
A. M. HOLTSLAG[2], JOAN CUXART[3], IGOR ESAU[4], JEAN-CHRISTOPHE
GOLAZ[5], MARIA A. JIMENEZ[3], MARAT KHAIROUTDINOV[6], BRANKO
KOSOVIC[7], DAVID LEWELLEN[8], THOMAS S. LUND[9], JULIE K.
LUNDQUIST[7], ANNE MCCABE[1], ARNOLD F. MOENE[2], YIGN NOH[10],
SIEGFRIED RAASCH[11] and PETER SULLIVAN[12]

[1] *Met Office, U.K.;* [2] *Wageningen University, The Netherlands;* [3] *Universitat de les Illes Balears, Spain;* [4] *Nansen Environmental and Remote Sensing Center, Norway;* [5] *National Research Council, Naval Research Laboratory, Monterey, CA, U.S.A.;* [6] *Colorado State University, U.S.A.;* [7] *Lawrence Livermore National Laboratory, U.S.A.;* [8] *West Virginia University, U.S.A.;* [9] *Colorado Research Associates, U.S.A.;* [10] *Yonsei University, South Korea;* [11] *University of Hannover, Germany;* [12] *National Center for Atmospheric Research, U.S.A.*

Abstract. Results are presented from the first intercomparison of large-eddy simulation (LES) models for the stable boundary layer (SBL), as part of the Global Energy and Water Cycle Experiment Atmospheric Boundary Layer Study initiative. A moderately stable case is used, based on Arctic observations. All models produce successful simulations, in as much as they generate resolved turbulence and reflect many of the results from local scaling theory and observations. Simulations performed at 1-m and 2-m resolution show only small changes in the mean profiles compared to coarser resolutions. Also, sensitivity to subgrid models for individual models highlights their importance in SBL simulation at moderate resolution (6.25 m). Stability functions are derived from the LES using typical mixing lengths used in numerical weather prediction (NWP) and climate models. The functions have smaller values than those used in NWP. There is also support for the use of K-profile similarity in parametrizations. Thus, the results provide improved understanding and motivate future developments of the parametrization of the SBL.

Keywords: Large-eddy simulation, Parametrization, Resolution, Stable boundary layer, Subgrid model.

1. Introduction

The large-eddy simulation (LES) of the stably stratified atmospheric boundary layer is a very challenging task. Whilst much progress has been made in simulating the convective cloudy boundary layer over the last decade (see Moeng et al., 1996; Brown et al., 2002 for recent intercomparison studies), progress with modelling the stable boundary layer (SBL) has been

* E-mail: bob.beare@metoffice.com

slower. One source of difficulty with the stable boundary layer and LES is that the characteristic eddies are much smaller than in the convective boundary layer, and thus require significantly more resolution and computer power for a reliable simulation. The small size of the eddies makes it much more difficult for the model to maintain resolved turbulence. When the resolution is coarse relative to the size of the eddies, or the subgrid model excessively dissipative, the subgrid fluxes dominate over the total and the resolved turbulence vanishes in scenarios where the forcings imply continuous turbulence. Although the subgrid model may still provide a reasonable model of the fluxes in these instances, the simulation is no longer a true LES. Those papers that have reported successful simulations (i.e., with resolved turbulence) are mainly for the weakly/moderately stable boundary layer: Mason and Derbyshire (1990), Brown et al. (1994), Andren (1995), Galmarini et al. (1998), Kosovic and Curry (2000) and Saiki et al. (2000). Most of these are reviewed by Beare and Mac Vean (2004).

Whilst the SBL is difficult for LES, the parametrization of the SBL in large-scale models is important for various aspects of numerical weather prediction (NWP) and climate modelling (Louis, 1979; Beljaars and Holtslag, 1991; King et al., 2001). Examples include: surface temperature forecasting over land at night, fog prediction, the timing of convection, and polar climate. Given the need to improve and understand the parametrization of SBLs in large-scale models, the Global Energy and Water Cycle Experiment Atmospheric Boundary Layer Study (GABLS) initiative was launched in 2002 (Holtslag, 2003). One question motivating this study was: why do climate models require more mixing in their SBL schemes relative to Monin–Obukhov theory and observations? Since LES has proved a useful guide for other physical parametrisations in the past, one component of the initiative was to perform the first intercomparison of large-eddy models for the SBL. This paper describes results from this component. The role of the intercomparison study was to assess the reliability and sensitivity of different models for an SBL case based on observations. This mirrored the approach of intercomparisons of the convective boundary layer, for example Moeng et al. (1996). Also, the results would provide further guidance for SBL parametrization.

In order to provide a useful test-case for intercomparison, the situation studied by Kosovic and Curry (2000) was chosen. This was adopted because it used initial conditions consistent with the BASE (Beaufort Sea Arctic Stratus Experiment) observations, was moderately stable $\left(\frac{h}{L} \sim 2\right.$, where h is the SBL height and L is the surface Obukhov length) and thus likely to be mainly continuously turbulent, and had previously been successfully simulated. The case, described more in Section 2, represents a typical quasi-equilibrium moderately stable boundary layer, akin to those commonly observed over polar regions and equilibrium nighttime conditions over land

in middle latitudes. Given that it was mainly a continuously turbulent case, it was then possible to compare this case against scalings derived from observations of other continuously turbulent SBLs, for example the results of Nieuwstadt (1984). It was appreciated from the outset that this was only one regime of the SBL, and others, such as the very stable nocturnal boundary layer, were also very important to understand for the parametrization problem. However, given the difficulty of large-eddy simulation of the SBL in the past, it was decided that the moderately stable case gave the best chance of success. Modelling the turbulence of the very stable boundary layer is a useful ultimate goal, but is beyond the scope of this work.

Using the moderately stable case (outlined in Section 2), we provide an overview of the output of different LES models (Section 3), assess the sensitivity to resolution and sub-grid scale model (Section 4), and compare the results with observations (Section 5), and typical first-order parametrizations used in NWP and climate models (Section 6). Finally, the results are discussed in Section 7, and conclusions made in Section 8.

2. Case Description

The case used here is based on Kosovic and Curry (2000), but adopting a slightly different wind initialisation. In a similar way to other intercomparisons (e.g., Moeng et al., 1996; Brown et al., 2002) , an initial state and forcings were used that are broadly based on an observational dataset, in this case the BASE Arctic observations.

The initial potential temperature profile consisted of a mixed layer (with potential temperature 265 K) up to 100 m with an overlying inversion of strength $0.01\,\mathrm{Km^{-1}}$. A prescribed surface cooling of $0.25\,\mathrm{K\,h^{-1}}$ was applied for 9 h so that a quasi-equilibrium state was approached. Time scales quoted for adjustment to quasi-equilibrium for this case differ: Beare and MacVean (2004) gave 9 h, but Kosovic and Curry (2004) stated a full inertial period of 12 h. Also, achievement of quasi-equilibrium depends on the quantity being examined. For the purposes of this work, it was defined as the time when the hour averaged mean wind reached a quasi-steady state. An assessment of how well this was achieved for the different models will be given in Section 4.

The geostrophic wind was set to 8 m s^{-1} in the east–west direction, with a Coriolis parameter of $1.39 \times 10^{-4}\,\mathrm{s^{-1}}$ (corresponding to latitude 73°N). The initial wind profile was geostrophic except at the bottom grid point where it was zero. In order to stimulate turbulence, a random potential temperature perturbation of amplitude 0.1 K and zero mean was applied below height 50 m. For models with a turbulent kinetic energy (TKE) subgrid closure, the TKE field was initialised as $0.4(1 - z/250)^3\mathrm{m^2\,s^{-2}}$, below a height ($z$) of 250 m.

The vertical velocity was set to zero at the surface and upper lid of the domain, and the upper boundary condition was free slip. To limit gravity-wave reflection at the top of the domain, most models applied gravity wave damping above 300 m. Monin–Obukhov similarity was applied at the bottom boundary (with recommended constants: $\beta_m = 4.8$ and $\beta_h = 7.8$) using a surface roughness length of 0.1 m for momentum and heat, and a von Karman constant (κ) of 0.4. The reference surface potential temperature was 263.5 K, density 1.3223 kg m^{-3}, gravity 9.81 m s^{-2}. The domain size was set to 400 m $\times$ 400 m $\times$ 400 m; Beare and MacVean (2004) found that doubling the horizontal domain size had a negligible effect for this case. However, it is acknowledged that the domain size was still too small to permit the majority of gravity waves that might be stimulated (domains significantly larger than 1 km would be required). Nevertheless, since the motivation of the study was to model SBL turbulence, this was not a severe restriction in this instance.

An isotropic grid was used, and simulations were performed at grid lengths of 12.5, 6.25, 3.125, 2, and 1 m, depending on the computer power and time available to the contributors. Profiles averaged over the horizontal domain and over the final and penultimate hours of the simulation were calculated; in general, the mean profile will refer to averages over the final hour, except when specified otherwise. Time series data were provided for the entire simulation. The boundary-layer depth (h) calculation involved first determining the height where the mean stress fell to 5% of its surface value ($h_{0.05}$) followed by linear extrapolation: $h = h_{0.05}/0.95$. This was the same method as used by Kosovic and Curry (2000), who gave a justification for calculating SBL height from the stress instead of heat flux.

Table I lists the participants and Table II summarises the models, giving the minimum grid length used and distinguishing the types of subgrid model and scalar advection scheme. This summary omits much of the detail of the for-mulations. For more detail, the reader should consult the references listed in Table III. As is evident, the configurations of the models do not permit a clean test of sensitivity to individual model components. However, some sensitivity tests were performed, varying the configuration constants for the individual subgrid models at moderate resolution. Whilst many participants were able to perform simulations down to a grid length of 3.125 m (Figure 1), only two were able to perform simulations at 1 m. This was because it required well over a month of state-of-the-art parallel supercomputer time to perform the calculation.

3. Overview

Large amounts of data were made available by the participants, not all of which it is possible to include here. Comprehensive details of the case and

TABLE I
A summary of the participants.

Model	Institution (s)	Scientist (s)
MO	Met Office, UK	Beare, McCabe, MacVean
CSU	Colorado State University	Khairoutdinov
IMUK	University of Hannover, Yonsei University	Raasch, Noh
LLNL	Lawrence Livermore National Laboratory	Lundquist, Kosovic
NERSC	Nansen Environment and Remote Sensing Center	Esau
WVU	West Virginia University	Lewellen
NCAR	National Center for Atmospheric Research	Sullivan
UIB	Universitat de les Illes Balears	Jimenez, Cuxart
CORA	Colorado Research Associates	Lund
WU	Wageningen University	Moene, Holtslag
COAMPS™	Naval Research Laboratory	Golaz

TABLE II
The minimum grid lengths and formulations used.

Model	Minimum grid length (m)	Scalar Advection	Sub-grid model
MO	1	TVD	Smagorinsky/backscatter
CSU	3.125	Monotone	TKE
IMUK	1	Piacsek–Williams	TKE
LLNL	3.125	Pseudospectral/differencing	Nonlinear two-part
NERSC	3.125	Central differencing	Dynamic mixed
WVU	6.25	Monotone	TKE with rotation effects
NCAR	2	Spectral horizontal/ monotone vertical	Two-part
UIB	2	Centred and positive definite	TKE
CORA	2	Spectral horizontal/ monotone vertical	Dynamic Smagorinsky
WU	6.25	Piacsek–Williams	TKE
COAMPS™	6.25	Positive definite	Smagorinsky

results are available online at www.gabls.org. Table IV gives a summary of the mean SBL heights for all simulations performed. Even simulations at 12.5-m resolution were successful, supported by fact that the boundary-layer depths were within 40% of the very high resolution (1 m) simulations. In the remainder of the section, an overview of the results is presented by showing plots at resolutions between 2 and 6.25 m, thus covering data from all participants and spanning a range of resolutions.

TABLE III
References for each of the models.

Model	References
MO	Brown et al. (1994) and Beare and Mac Vean (2004)
CSU	Khairoutdinov and Randall (2003)
IMUK	Raash and Etling (1991) and Raash and Schröter (2001)
LLNL	Kosovic (1997)
NERSC	Esau (2004)
WVU	Lewellen and Lewellen (1998) and Lewellen et al. (2000)
NCAR	Sullivan et al. (1994) and Koren (1993)
UIB	Cuxart et al. (2000)
CORA	See NCAR
WU	Cuijpers and Duynkerke (1993) and Dosio et al. (2003)
COAMPS^{TM}	Hodur (1997)

Figure 1. Key to lines representing different participating models.

Mean profiles of the potential temperature, wind speed, buoyancy flux and momentum flux are shown in Figures 2–5, respectively. The profiles exhibit a positive curvature in the potential temperature near the top of the SBL, a pronounced super-geostrophic jet peaking near the top of the boundary layer, and linear buoyancy flux profiles. These features are consistent with the theoretical one-dimensional model of Nieuwstadt (1985). The model assumes equilibrium conditions with a constant Richardson number closure and predicts a super-geostrophic jet with a momentum balance between the Coriolis force and vertical divergence of momentum flux. The spread in Figures 2–5 is not surprising given the sensitivity of previous SBL simulations to model configuration (see, for example, Brown et al., 1994) . Given the difficulty of the large-eddy simulation of the SBL in the past, a notable success here is that the spread was not any larger.

The main differences in the mean potential temperature and wind profiles occur towards the top of the boundary layer (Figures 2 and 3). There are fewer differences lower down due to the fact that the surface boundary condition prescribes both the surface temperature and the wind. However,

TABLE IV

Boundary-layer heights (in metres) for last hour of simulation and each of the models at different resolutions.

Model/resolution	1 m	2 m	3.125 m	6.25 m	12.5 m
MO	164	162	171	204	263
CSU	–	–	197	211	237
IMUK	149	162	168	158	–
LLNL	–	–	169	194	257
NERSC	–	–	179	188	204
WVU	–	–	–	201	197
NCAR	–	197	204	–	–
UIB	–	163	173	174	191
CORA	–	187	195	211	–
WU	–	–	–	178	158
COAMPS^{TM}	–	–	–	161	–
ENSEMBLE MEAN	157	174	182	188	215

the behaviour of the LLNL simulation at 6.25-m resolution is quite different at the surface suggesting differences in the application of the surface boundary conditions. In addition to boundary-layer depth, there are differences in the potential temperature profiles at the top of the SBL where they blend with the overlying inversion. In the wind speed, a spread can be seen in both the magnitude and height of the nocturnal jet. Even at 2-m resolution, there is a range of results, with the NCAR and CORA models favouring deeper, more turbulent SBLs relative to IMUK and MO, and UIB in the middle. The split corresponds to IMUK and MO having lower surface momentum and heat fluxes relative to both NCAR and CORA. Also, for a moderately stable situation such as this, scaling implies intermittence at the SBL top (Holtslag and Nieuwstadt, 1986). This may also contribute to variability in SBL depth.

There is more spread in the mean buoyancy and momentum flux profiles (Figures 4 and 5), throughout the boundary layer; the surface boundary conditions allow differences at the surface. At the surface, the mean buoyancy fluxes are -3.5 to $-5.5 \times 10^{-4} \, \text{m}^2 \, \text{s}^{-3}$, corresponding to a heat flux of -12.5 to $-19.6 \, \text{W m}^{-2}$, and the magnitude of the mean momentum fluxes are 0.06–$0.08 \, \text{m}^2 \, \text{s}^{-2}$, corresponding to a friction velocity of 0.24–$0.28 \, \text{m s}^{-1}$. These values are within the range of surface heat fluxes (-5.7 to $-48.4 \, \text{W m}^{-2}$) and friction velocities (0.22–$0.59 \, \text{m s}^{-1}$) for continuously turbulent SBLs observed in the CASES-99 experiment (Poulos et al., 2002; Van de Wiel et al., 2003). However, they are slightly above the range of
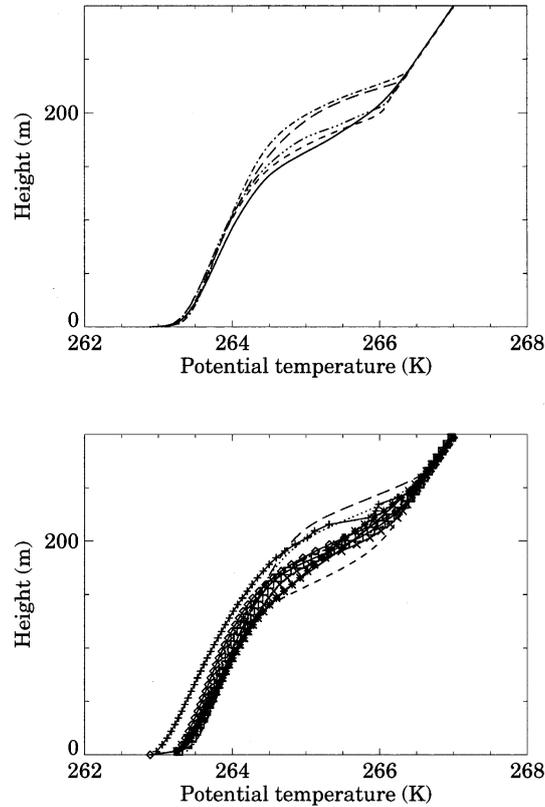
Figure 2. Mean profiles of potential temperature at resolutions of 2 m (top) and 6.25 m (bottom).

observations from the SHEBA Arctic experiment with typical surface heat fluxes in the range of -2 to $-8\,\mathrm{Wm^{-2}}$ and friction velocities in the range 0.15–$0.2\,\mathrm{ms^{-1}}$ (Persson et al., 2002). This may be partly due to the fact that, although the initial conditions were consistent with Arctic observations, the surface cooling was more idealized.

Figure 6 shows time series of the surface momentum and buoyancy flux and the SBL depth at 3.125-m resolution. Again, there is spread between models. The momentum fluxes reach a quasi-equilibrium value after about $1.5 \times 10^4\,\mathrm{s}$ (4 h), but the SBL depth equilibrates within only $0.5 \times 10^4\,\mathrm{s}$ (1.5 h). The surface buoyancy flux is still changing slightly at 9 h this is consistent with the fact that the surface boundary condition is a cooling rate as opposed to a flux condition. There is significant variability in the boundary-layer depth, fluctuating between about 150 and 200 m up until 9 h. This is consistent with intermittency at the SBL top (Holtslag and Nieuwstadt, 1986).
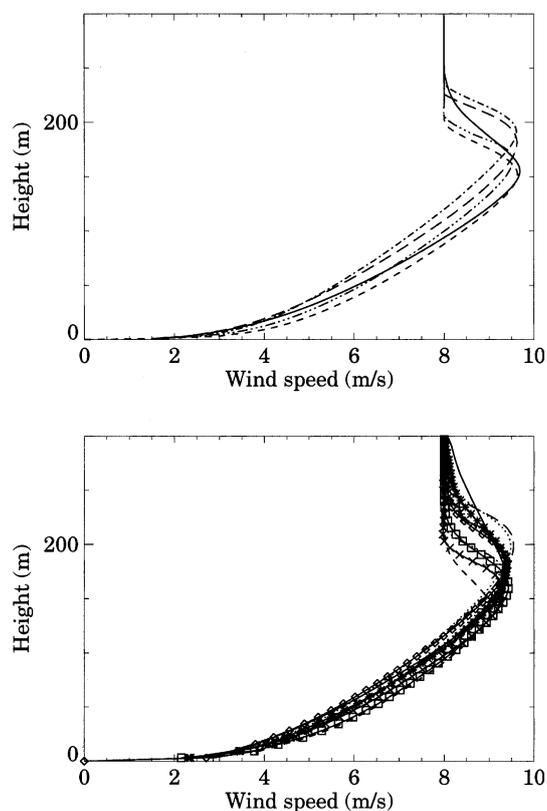
Figure 3. Mean profiles of wind speed at resolutions of 2 m (top) and 6.25 m (bottom).

4. Model Sensitivity Tests

Two critical tests of a LES are that its mean statistics are robust with increasing resolution, and are reasonably insensitive to subgrid model (see, for example, Mason, 1994). Until very recently (Beare and Mac Vean, 2004), there has been insufficient computer power to perform this test for the SBL. However, in this intercomparison, several of the participants were able to provide simulations over a range of resolutions and also use different subgrid models.

4.1. Sensitivity to resolution

Ideally LESs should be at a grid length below which the mean statistics are stationary with increasing resolution. However, the results thus far have indicated that reasonable results are still achievable when this limit has not been reached. Table IV shows that the ensemble mean boundary-layer height
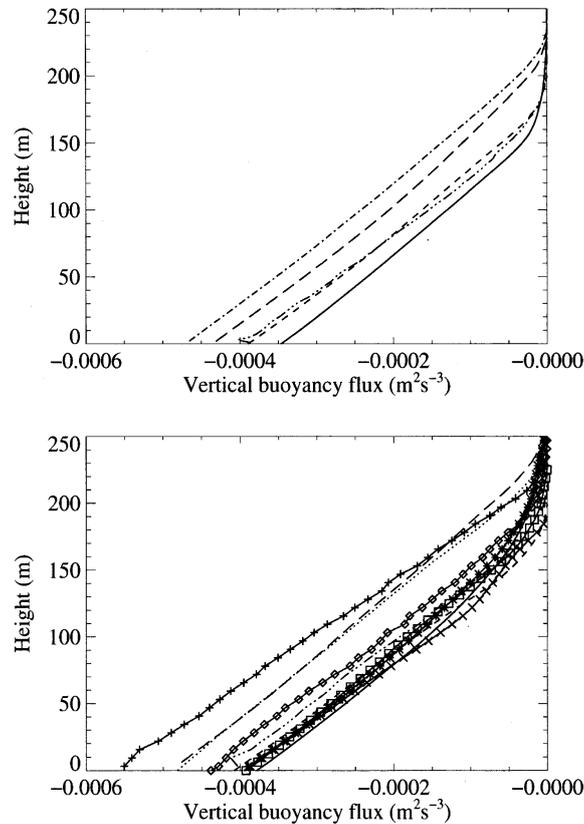
Figure 4. Mean profiles of buoyancy flux at resolutions of 2 m (top) and 6.25 m (bottom).

at 12.5-m resolution is within 40% of the 1-m resolution result and at 6.25-m resolution it is within 20%. The remainder of the section explores the degree to which the ideal limit of stationarity with increased resolution can be reached.

Sensitivity to resolution perhaps has most meaning for simulations that have reached a quasi-equilibrium state. Although there is no universal definition for quasi-equilibrium, this was assessed by taking the root-mean-square difference in the wind speed averaged over 7–8 h and 8–9 h. This difference was smaller than $0.1\,\mathrm{m\,s^{-1}}$ for all simulations, so a reasonable quasi-steady state was considered to have been achieved. Nevertheless, small changes in the potential temperature inversion at the SBL top were observed by LLNL with integration beyond 9 h (Kosovic per. com.).

Figure 7 shows the mean potential temperature and wind speeds for those models with three or more simulations at different resolutions down to a grid length of 2 m or less. The MO model shows a general decrease of
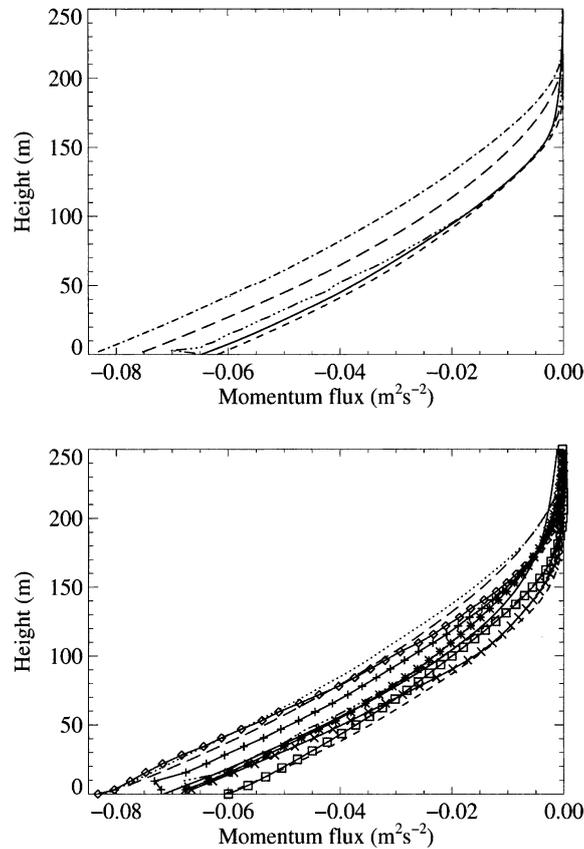
Figure 5. Mean profiles of momentum flux at resolutions of 2 m (top) and 6.25 m (bottom).

boundary-layer depth, an enhancement of positive curvature in potential temperature in the interior of the SBL, and increase of jet strength with increased resolution. For grid lengths of 3.125 m or less, the profiles are closer than the profiles at larger grid lengths. For IMUK, the profiles are similar below 3.125-m resolution, and the 6.25-m resolution run exhibits a lower boundary layer than the high resolution runs. This feature is possibly related to the different subgrid models used. MO uses backscatter, which enhances the boundary-layer depth in marginally resolved situations (Brown et al., 1994), while IMUK uses a TKE subgrid model (see Table II). The 6.25-m IMUK simulation thus mimics the potential temperature profiles at higher resolution although not the wind speed. For CORA, the 6.25-m resolution profiles are much closer to the higher resolution ones. However, no CORA simulations of 1 m were performed so at this resolution no comparison can be made with the IMUK and MO results. For UIB, the potential temperature profiles are close over the
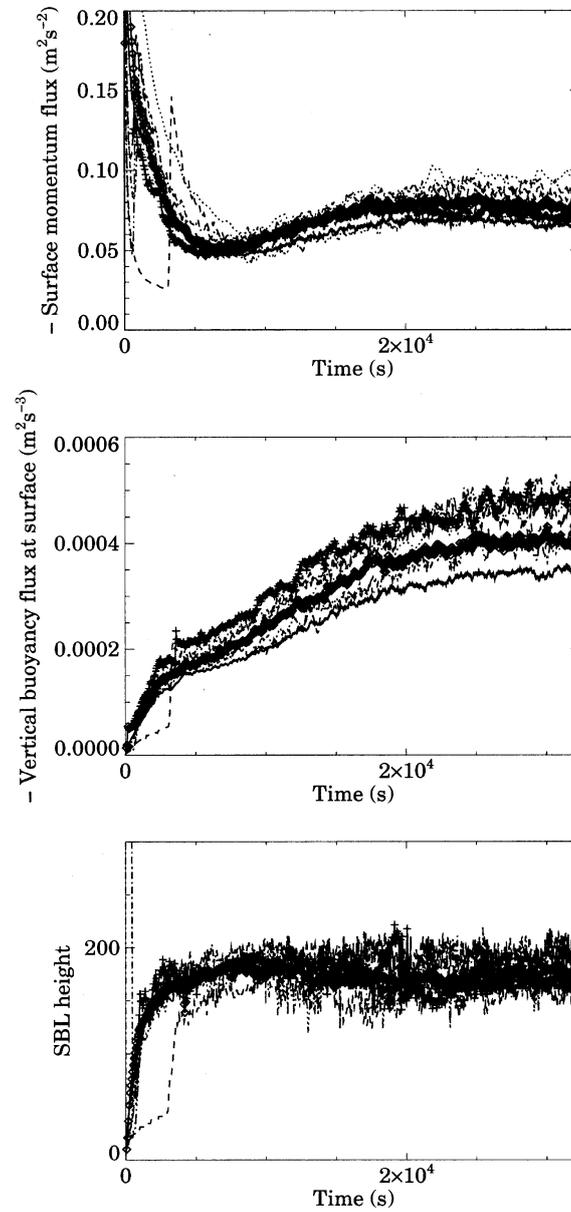
Figure 6. Time series for surface momentum flux, surface buoyancy flux and boundary layer height for 3.125-m resolution.

different resolutions, but there is more resolution sensitivity in the wind speeds.

There are still small changes near the top of the boundary layer below 3.125-m resolution. However, these changes are qualitatively comparable
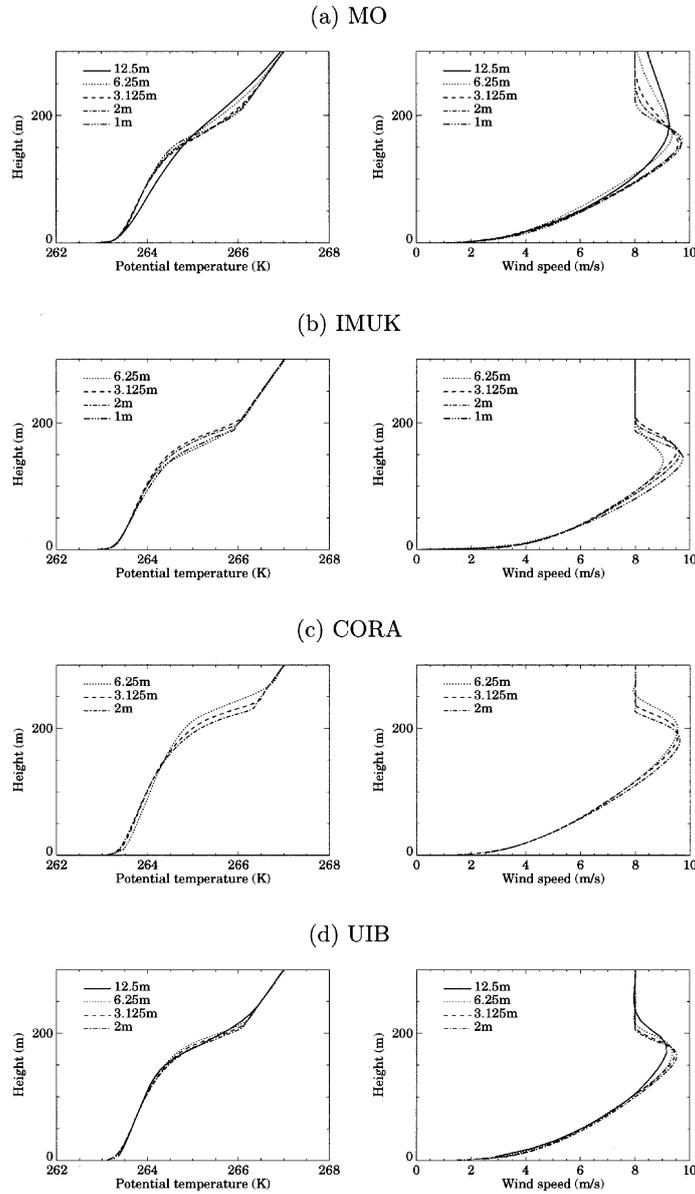
(a) MO

(b) IMUK

(c) CORA

(d) UIB

Figure 7. Mean potential temperature and wind speed at different resolutions, for models with three or more simulations down to 2 m or less.

to those found by Brown (1999) for the mean statistics of the cumulus capped boundary layer at 20-m resolution, with the conclusion that their relative insensitivity to model resolution indicated their robustness. The changes at this very high resolution are also arguably considerably smaller

than the sensitivity of the underlying flow, for example the strong dependence of the boundary-layer depth on surface fluxes. Thus, although absolute convergence has not been demonstrated and might require more computer power, the robustness of the results below 3.125-m resolution is clear.

4.2. SENSITIVITY TO SUB-GRID MODEL

Some participants provided sensitivity tests to sub-grid model formulation and configuration, shown in Figure 8. LLNL gave results from three different types of sub-grid model: nonlinear Deardorff (nonlinear model with prognostic sub-grid TKE), nonlinear Smagorinsky, and Smagorinsky (Kosovic, 1997). There are differences towards the top of the boundary layer, and in the curvature of the potential temperature profile in the transition to the overlying layer. Comparisons for MO are shown for the Smagorinsky sub-grid model, with and without backscatter, and for different values of the Smagorinsky parameter, C_s, the ratio of the basic mixing length to horizontal grid length. Following Lilly (1967), the sub-grid dissipation is proportional to $(C_s\Delta)^2$, where Δ is the grid length. Thus, higher values of C_s give higher levels of sub-grid dissipation. Values of C_s are not directly comparable between the Smagorinsky model with and without backscatter since backscatter serves to scatter energy from the sub-grid scales back onto the resolved scales (Beare and MacVean, 2004). Again, differences can be seen towards the top of the boundary layer. The backscatter simulation with $C_s = 0.23$ has a shallower boundary layer than the equivalent run with $C_s = 0.15$. The increased dissipation of the sub-grid model in the former case apparently dampens down the turbulence, and thus reduces the boundary-layer height. The sensitivity of the NERSC and MO model is shown using the Smagorinsky model with increasing C_s. With the C_s value of 0.23, the SBL has lost most of its structure in potential temperature for both models, giving evidence of vanishing of the resolved turbulence. Thus, the C_s value of 0.23 is probably too large for use with the Smagorinsky model alone at 6.25-m resolution. Using the dynamic Smagorinsky scheme (Esau, 2004), the NERSC model maintains a deeper SBL. The spread in the mean profiles in Figure 8 is similar to that in Figure 2 for 6.25-m resolution, suggesting that the differences there may be largely attributable to the sub-grid model.

Although these results are useful in discriminating models and consistent with previous findings (e.g., Brown et al., 1994), they do bring into question the reliability of simulation of this SBL case at 6.25-m resolution. Ideally, reasonable insensitivity to sub-grid model needs to be demonstrated (Mason, 1994). Sensitivity tests to switching backscatter on and off at 1-m resolution were performed for the MO model (Figure 9). The difference between
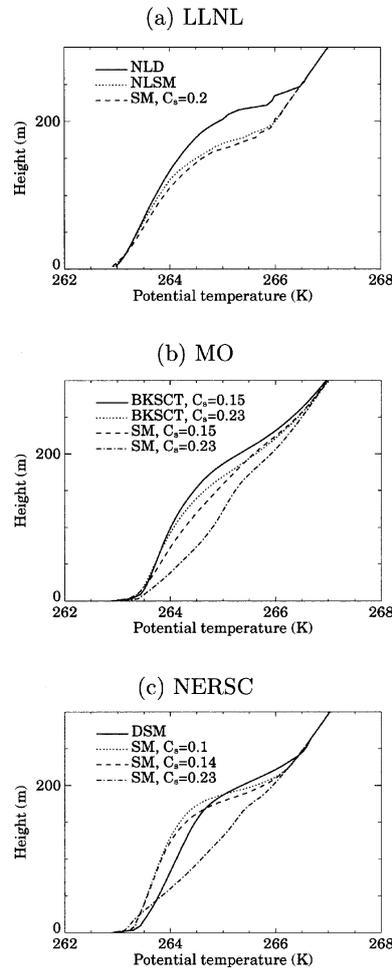
(a) LLNL

(b) MO

(c) NERSC

Figure 8. Mean potential temperature with different sub-grid model configurations and formulations (NLD and NLSM are non-linear Deardorf and Smagorinsky, BKSCT is stochastic backscatter, SM is Smagorinsky and DSM is Dynamic Smagorinsky) for resolution 6.25 m.

profiles, although not non-zero at the top of the boundary layer, are considerably reduced relative to the 6.25-m resolution results. Thus, at sufficiently high resolution, the simpler Smagorinsky model (backscatter off) is just as effective as the Backscatter model.

5. Comparison with Observations

An additional test of the reliability of the LES was to compare the results against published observations. Brief comparisons with the surface data from
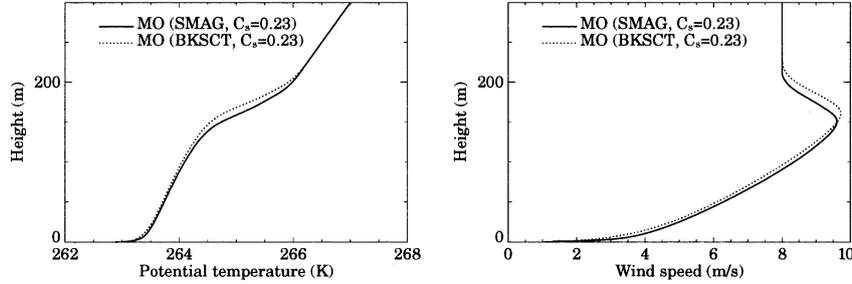
Figure 9. Mean potential temperature and wind speed with and without backscatter in the MO model at resolution 1 m.

CASES-99 and SHEBA were made in Section 3. Here the comparison is extended to include vertical profiles. Although the simulations were initialised with a profile based on observations, the constant surface cooling boundary condition was an idealisation. Thus, the most effective method for comparison of vertical profiles with observations was to non-dimensionalise the data.

The LES data were compared against the observations of Nieuwstadt for the Cabauw meteorological mast in the Netherlands, collected over a time period from September 1977 to February 1979. The site had approximately flat terrain and data selection was applied so that the observed turbulence was continuous (when the geostrophic wind was greater than 5 m s^{-1}) and in a quasi-equilibrium state [by starting observations about 2–3 hours after sunset, further details are in Nieuwstadt (1984)]. The observational conditions were thus analogous to those of the LES at final time.

Effective diffusivities of momentum ($K_{\mathrm{m}}^{\mathrm{eff}}$) and heat ($K_{\mathrm{h}}^{\mathrm{eff}}$) were calculated from the total momentum and heat fluxes and the mean wind and potential temperature profiles. For example, the effective momentum diffusion of the LES was calculated using the total momentum fluxes, and using the wind shear from mean LES winds (U,V):

$$K_{\mathrm{m}}^{\mathrm{eff}} = \frac{\tau}{\left(\frac{\partial U^2}{\partial z} + \frac{\partial V^2}{\partial z}\right)^{\frac{1}{2}}}. \tag{1}$$

Following Nieuwstadt (1984), they were then non-dimensionalised using

$$\phi_{KM} = \frac{K_{\mathrm{m}}^{\mathrm{eff}}}{\Lambda \tau^{\frac{1}{2}}} \quad \text{and} \quad \phi_{KH} = \frac{K_{\mathrm{h}}^{\mathrm{eff}}}{\Lambda \tau^{\frac{1}{2}}}, \tag{2}$$

respectively, where Λ is the *local* Obukhov length, $\Lambda = -\tau^{\frac{3}{2}}/\kappa\overline{wb}$, τ is the mean total (resolved plus sub-grid) vertical momentum flux, and $\overline{wb}$ is the mean total vertical buoyancy flux. The local scaling theory of Nieuwstadt

(1984) states that these non-dimensional diffusivities can be expressed solely as functions of z/Λ, and for large z/Λ will approach a constant value (z-less scaling).

Figure 10 shows ϕ_{KM} and ϕ_{KH} against z/Λ at 2 and 6.25 m resolutions, along with the scaled observations of Nieuwstadt (1984) and their standard deviation. Even at 6.25-m resolution, the ϕ_{KM} profiles reach an approximately constant value at large z/Λ, consistent with local scaling. However, at this resolution about half of the LES results imply greater non-dimensional momentum diffusion than the observations. The ϕ_{KH} profiles have considerably more spread at 6.25-m resolution, and only four of the profiles pass through the observation range. At 2-m resolution, however, all the ϕ_{KM} profiles pass through the range of the observations at large z/Λ, but still overestimate the values relative to observations at small z/Λ. This provides additional evidence that high resolution is required for reliable LES of the SBL. There is still a spread in ϕ_{KM} and ϕ_{KH} at 2-m resolution with the MO model implying less heat and momentum diffusion than the others; this difference is less than the observational error, however. The results of IMUK and MO at 1 m (not shown) favoured the lower limiting values of ϕ_{KM} between 0.06 and 0.08.
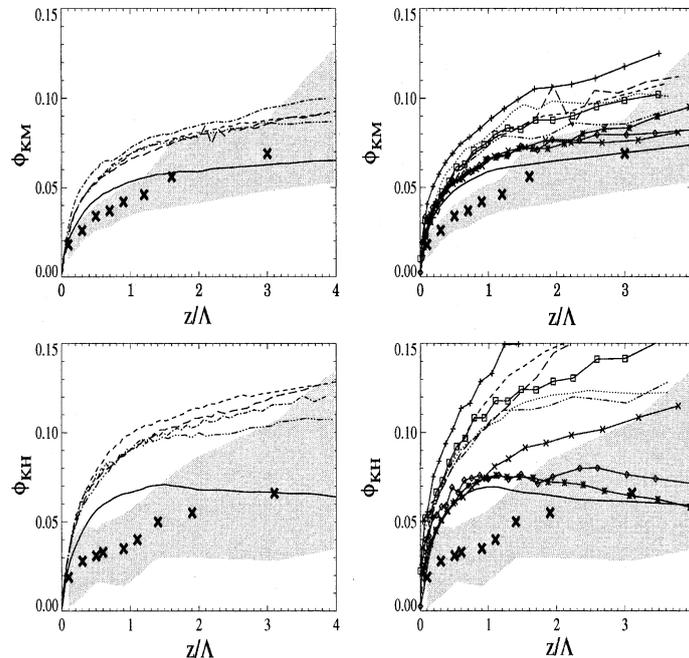

Figure 10. Locally scaled momentum (top) and heat (bottom) diffusivities compared with the Nieuwstadt (1984) observations (crosses for mean values and the grey shaded areas giving the standard deviation) for resolutions of 2 m (left column) and 6.25 m (right column).

The theoretical model of Nieuwstadt (1985) predicts the following similarity profiles for mean buoyancy and momentum flux:

$$\frac{\overline{wb}}{\overline{wb}_0} = \left(1 - \frac{z}{h}\right)^{m_{w\theta}} \tag{3a}$$

$$\frac{\tau}{\tau_0} = \left(1 - \frac{z}{h}\right)^{m_\tau}, \tag{3b}$$

where the subscript 0 indicates the surface values. The analysis of Nieuwstadt (1985) gives the following values for the exponents: $m_{w\theta} = 1$, $m_\tau = 1.5$.

Figure 11 compares the normalised mean momentum and heat fluxes of the LES with the profiles in Equation (3) and also the observations of Nieuwstadt (1984). At both 6.25-m and 2-m resolution, the normalised profiles have a much smaller spread than the standard deviation of the observations, and lie close to the mean observations and the theoretical profiles in (3). The fact that the normalised fluxes have much less spread compared with the
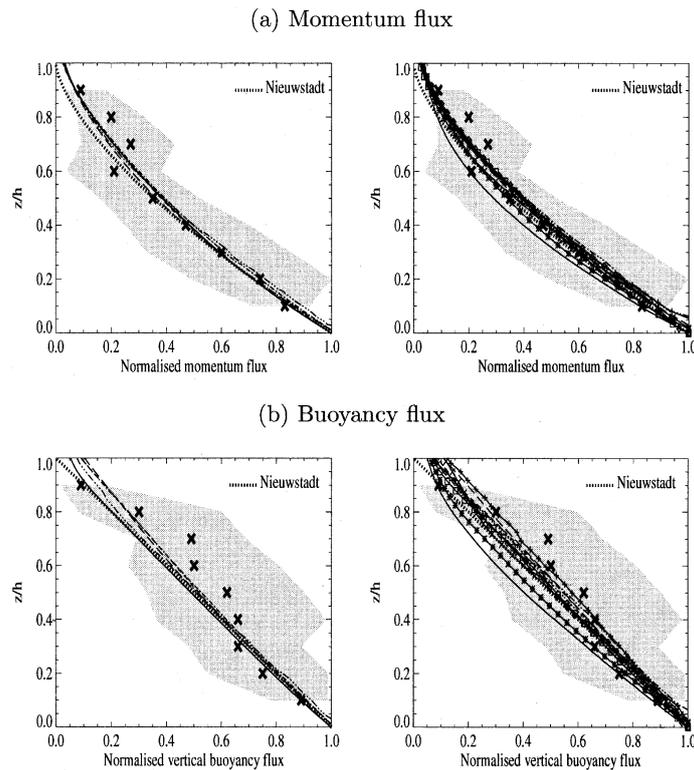
(a) Momentum flux

(b) Buoyancy flux

Figure 11. (a) Momentum flux and (b) buoyancy flux normalised by surface values plotted against height normalised by boundary layer depth for resolution 2 m (left column) and 6.25 m (right column). Mean observations of Nieuwstadt (1984) shown as crosses, with standard deviation as shaded area. Theoretical profile of Nieuwstadt (1985) shown as dotted line.

non-normalised fluxes in Figures 4 and 5, indicates that much of the spread is due to variations in the boundary-layer depth and surface fluxes.

6. Comparison with First-order Parametrisations

One of the questions motivating the GABLS initiative was: why do climate models require more mixing in their SBL schemes relative to Monin–Obukhov theory and observations (Holtslag, 2003)? This question is addressed here in light of the LES results. First-order parametrisations of the SBL are often used in operational NWP and climate models, following, for example, Louis (1979). These express the parametrised vertical diffusivities of momentum (K_m) and heat (K_h) as functions of mixing length (λ), vertical wind shear (S), and functions of gradient Richardson number (Ri):

$$K_m = \lambda^2 S f_m(Ri) \quad \text{and} \quad K_h = \lambda^2 S f_h(Ri). \tag{4}$$

For this study, a set-up similar to that used in the Met Office Unified Model (global configuration) is compared with the LES, since it is typical of others used in NWP. The mixing length is defined as:

$$\frac{1}{\lambda} = \frac{1}{\kappa(z + z_0)} + \frac{1}{\lambda_0} \; ; \quad \lambda_0 = 40\,\text{m}. \tag{5}$$

Much of the tuning of this scheme for use in NWP and climate involves adjusting the stability functions (f_m and f_h) such that they decrease with varying rates with increasing Richardson number. The asymptotic mixing length (λ_0) is also a tunable parameter. The stability functions typically used in operational models (e.g., Beljaars and Holtslag, 1991) are similar to the long-tails function, so-called for the relatively small fall off with Richardson number, while those used in research (e.g., King et al., 2001) are sometimes represented by the sharp function. The long-tails function has the form:

$$f_m(Ri) = \frac{1}{1 + 10Ri} \qquad Ri \geq 0. \tag{6}$$

The sharp form is given by:

$$f_m(Ri) = \begin{cases} (1 - 5Ri)^2 & 0 \leq Ri < 0.1 \\ \left(\frac{1}{20Ri}\right)^2 & Ri \geq 0.1. \end{cases} \tag{7}$$

Using Equations (4) and (5), an effective stability function ($f_{\text{les}}(Ri)$) was derived:

$$f_{\text{les}}(Ri) = \frac{K_m^{\text{eff}}}{\lambda_l^2 S}. \tag{8}$$

This definition is dependent on the mixing length used for the LES (λ_l) as well as the effective diffusion. Initially, the same mixing length was assumed as is used in the NWP parametrisation ($\lambda_l = \lambda$). This is still a fairly arbitrary definition, so sensitivity to mixing length was also considered.

Figure 12 shows the long-tails and sharp functions compared with the LES simulations of the momentum Richardson number functions for 6.25-m and 2-m resolutions. Typically, the LES simulations are much closer to the sharp profile than the long tails; from this evidence, the LES thus implies less mixing than typically used in operational NWP and climate models. At 2-m resolution, the LES Richardson number functions tend to have an even sharper cut off than at 6.25-m resolution. One reason for the difference is that the shallow SBL is often poorly resolved in NWP models. The Richardson numbers calculated at poor resolution might be larger than those for the fully resolved flow, and thus the stability function needs to decrease less rapidly with increasing Richardson number.
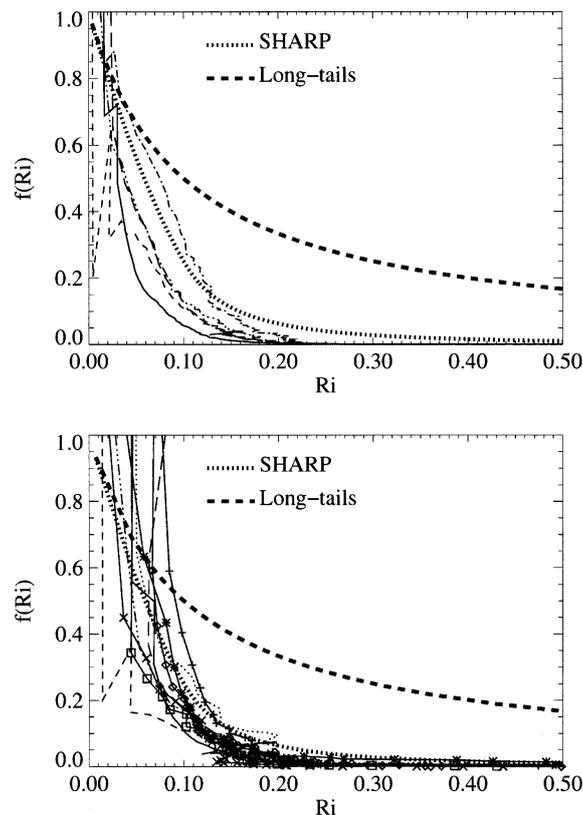

Figure 12. Effective momentum Richardson number stability functions compared with the long-tails and sharp functions for resolutions of 2 m (top) and 6.25 m (bottom).

The previous analysis assumed an asymptotic mixing length of 40 m. Figure 13 shows the implied stability functions for the ensemble mean of the 3.125-m simulations using asymptotic mixing lengths between 5 and 40 m. The implied stability function varies significantly with mixing length, increasing for smaller values. For an asymptotic mixing length of 5 m, the stability function is greater than the long-tails function for Richardson numbers less than 0.23. Thus, the statement of the LES implying less mixing than used in NWP appears only to have meaning in the context of the mixing length used in the comparison. Nevertheless, since the local Obukhov length in the interior of the SBL was of order 30–70 m, the 40 m asymptotic mixing length is arguably the most appropriate.

Another common form of first-order parametrisation is the K-profile type examined first by Brost and Wyngaard (1978), used in a simple model by Troen and Mahrt (1986) and compared with LES simulations by Holtslag (1998). The diffusion coefficients used by Brost and Wyngaard (1978) were:

$$\frac{K_{\mathrm{m}}}{u_*\mathrm{h}} = \frac{K_{\mathrm{h}}}{1.2u_*\mathrm{h}} = \frac{\kappa z}{\mathrm{h}}\frac{\left(1 - \frac{z}{\mathrm{h}}\right)^{1.5}}{1 + 4.7\frac{z}{L}} \tag{9}$$

where u_* is the friction velocity. Compared to Equation (4), Equation (9) replaces mixing lengths and stability functions with a diagnosis of SBL height. Figure 14 compares the normalised effective diffusions for the 6.25-m resolution runs with (9). Profiles for normalised momentum and heat diffusion are close and cluster fairly evenly around the profile given by (9). There is more spread in the normalised heat diffusion, but the profiles are still much closer than found by Holtslag (1998) when comparing with some LES data not near quasi-equilibrium. The usefulness of this parametrisation in practice
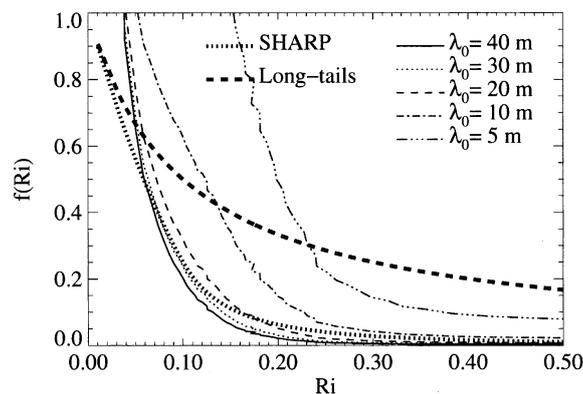

Figure 13. Effective momentum Richardson number stability functions compared with the long-tails and sharp functions for the ensemble mean at resolution 3.125 m for different asymptotic mixing lengths.
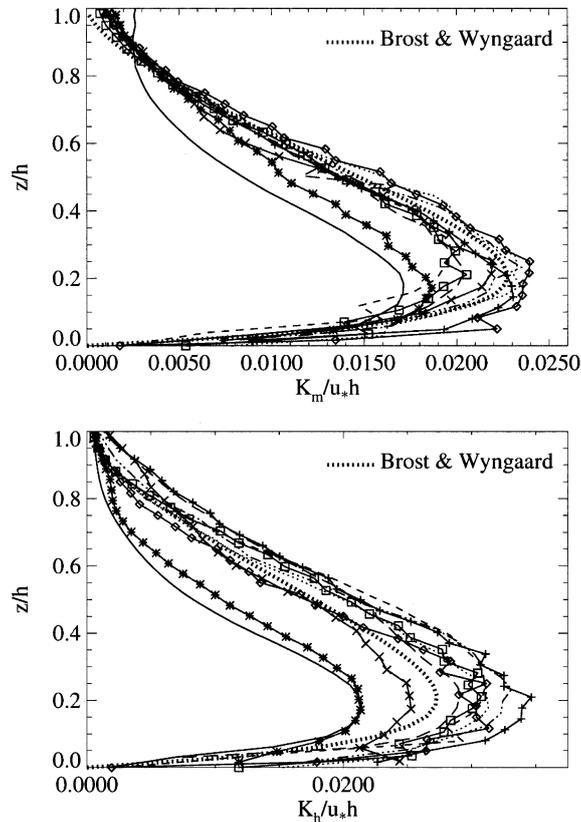
Figure 14. Effective momentum and heat diffusions normalised by SBL depth and friction velocity plotted against height normalised by SBL depth for simulations at 6.25-m resolution. Also shown are profiles of Brost and Wyngaard (1978).

is also dependent on an accurate diagnosis of SBL height (Vogelezang and Holtslag, 1996).

7. Discussion

The case studied here is only one type of stable boundary layer, although an important one, since the high latitude oceans will always prevent a strongly stratified SBL developing. Another is the very stable nocturnal boundary layer over land. This type can often have intermittent turbulence or even no turbulence (see, for example, Van de Wiel et al., 2003). Although it would be ideal to simulate this regime in the future, given the amount of computer power required for reliable LES of the moderately stable case, one should approach it carefully, gradually increasing the stratification. Also, the

observed nocturnal stable boundary layer over land has periods of transition to and from the convective boundary layer in the morning and evening respectively (see Grant, 1997; Grimsdell and Angevine, 2002). During these transition periods, conditions are often far from the quasi-equilibrium ones considered here.

One question motivating GABLS was: why do climate models require more mixing in their SBL schemes relative to Monin–Obukhov theory and observations? Here it was shown that the implied mixing functions from the LES were much less than that typically used in NWP and climate models, when using asymptotic mixing lengths typically used in NWP. The LES is thus in agreement with Monin–Obukhov theory and observations. The results provide a basis for future parametrisation developments. Bridging the gap between the stability functions and mixing lengths used in coarse resolution NWP and climate models and those derived from high resolution LES is an important issue. The high resolution LES also provides a limit to which the NWP models should converge when operated at much higher resolution in the future. Other important issues include: heterogeneity (Mahrt, 1987), intermittency, non-equilibrium effects, and compensating errors from other sections of the NWP system. The LES data also provide support for K-profile similarity functions (Brost and Wyngaard, 1978), provided an appropriate diagnosis of SBL height is used.

8. Conclusions

This paper presented results from the first intercomparison of LES of the stable boundary layer as part of the GABLS initiative. Using a moderately stable case inspired by the BASE Arctic observations, the outputs from eleven LES models were compared for a range of resolutions. A more complete picture of reliability and sensitivity that could be provided by one model was thus gained. It was demonstrated that simulation of the SBL is reliable for a quasi-equilibrium moderately stable case. At grid lengths of 12.5 m and less, the simulations were successful in sustaining resolved turbulence, and below a grid length of 3.125 m the mean statistics changed by a small amount. Thus, a grid length of 3.125 m or less is ideal for a robust LES of this moderately stable regime, but a grid length of 6.25 m will still produce a simulation with a reasonable (of order 20%) accuracy relative to the very high resolution simulations. Also, if just the Smagorinsky sub-grid model is used, a value of Smagorinsky constant of less than 0.2 is desirable. The results for this case could provide a standard dataset for other LES modellers to compare against when configuring their models for SBLs.

Sensitivity tests were performed for some of the models at moderate and high resolution. At moderate resolution (6.25 m), a similar spread in the

mean profiles for eleven models could be achieved with three models using different configurations of sub-grid model. The more sophisticated sub-grid models (e.g., non-linear Deardorf, stochastic backscatter and dynamic Smagorinsky) tended to be more effective at sustaining deeper SBLs relative to the Smagorinsky model at a grid length of 6.25 m, but the results became independent of sub-grid model at 1-m resolution. Given the computational expense of the very high resolution simulations, the sub-grid model is likely to continue to have an important role in future SBL simulations, especially in simulations of higher stability. There was reasonably good agreement between the high resolution LES results and the locally scaled observations of Nieuwstadt (1984) in the z-less limit. Non-dimensionalising the fluxes with respect to the surface fluxes and the boundary-layer depth significantly reduced the spread between the models to much less than the standard deviation of the observations of Nieuwstadt (1984); this indicated that the spread between them was mainly due to differences in surface fluxes and boundary-layer depth.

Acknowledgements

References

Andren, A.: 1995, 'The Structure of Stably Stratified Atmospheric Boundary Layes: A Large-Eddy Simulation Study', *Quart. J. Roy. Meteorol. Soc.* **121**, 961–985.

Beare, R. J. and MacVean, M. K.: 2004, 'Resolution Sensitivity and Scaling of Large-Eddy Simulations of the Stable Boundary Layer', *Boundary-Layer Meteorol.* **112,** 257–281.

Beljaars, A. C. M. and Holtslag A. A. M.: 1991, Flux Parameterization Over Land Surfaces for Atmospheric Models', *J. Appl. Meteorol.* **30**, 327–341.

Brost, R. A. and Wyngaard, J. C.: 1978, 'A Model Study of the Stably Stratified Planetary Boundary Layer', *J. Atmos. Sci.* **35**, 1427–1440.

Brown, A. R.: 1999, 'The Sensitivity of Large-Eddy Simulations of Shallow Cumulus Convection to Resolution and Subgrid Model', *Quart. J. Roy. Meteorol. Soc.* **125**, 469–482.

Brown, A. R., Cederwall, R. T., Chlond, A., Duynkerke, P., Golaz, J.-C., Khairoutdinov, M., Lewellen, D. C., Lock, A. P., MacVean, M. K., Moeng, C.-H., Neggers, R. A. J., Siebesma, A. P., and Stevens, B.: 2002, 'Large-Eddy Simulation of the Diurnal Cycle of Shallow Cumulus Convection Over Land', *Quart. J. Roy. Meteorol. Soc.* **128**, 1075–1093.

Brown, A. R., Derbyshire, S. H., and Mason, P. J.: 1994, 'Large-Eddy Simulation of Stable Atmospheric Boundary Layers with a Revised Stochastic Subgrid Model', *Quart. J. Roy. Meteorol. Soc.* **120**, 1485–1512.

Cuijpers, J. W. M. and Duynkerke, P. G.: 1993, 'Large Eddy Simulation of Trade Wind Cumulus Clouds', *J. Atmos. Sci.* **50**, 3894–3908.

Cuxart, J., Bougeault, P., and Redelsperger, J. L.: 2000, 'A Turbulence Scheme Allowing for Mesoscale and Large-Eddy Simulations', *Quart. J. Roy. Meteorol. Soc.* **126**, 1–30.

Dosio, A., de Arellano, J. V. G., Holtslag, A. A. M., and Builtjes, P. J. H.: 2003, 'Dispersion of a Passive Tracer in Buoyancy- and Shear-Driven Boundary Layers', *J. Appl. Meteorol.* **42**, 1116–1130.

Esau, I.: 2004, 'Simulation of Ekman Boundary Layers by Large Eddy Model with Dynamic Mixed Subfilter Closure', *J. Environ. Fluid Mech.* **4**, in press.

Galmarini, S., Beets, C., Duynkerke, P. G., and de Arellano, J. V.-G.: 1998, 'Stable Nocturnal Boundary Layers: a Comparison of One-dimensional and Large-Eddy Simulation Models', *Boundary-Layer Meteorol.* **88**, 181–210.

Grant, A. L. M.: 1997, 'An Observational Study of the Evening Transition Boundary-layer', *Quart. J. Roy. Meteorol. Soc.* **123**, 657–677.

Grimsdell, A. W. and Angevine, W. M.: 2002, 'Observations of the Afternoon Transition of the Convective Boundary Layer', *J. Appl. Meteorol.* **41**, 3–11.

Hodur, R. M.: 1997, 'The Naval Research Laboratory's Coupled Ocean/Atmosphere Meso-Scale Prediction System (COAMPS)', *Mon. Wea. Rev.* **117**, 1414–1430.

Holtslag, A. A. M.: 1998, 'Modelling Atmospheric Boundary Layers', in A. A. M. Holtslag and P. G. Duynkerke, (eds.), *Clear and Cloudy Boundary Layers, Proceedings of the Academy colloquim held in Amsterdam, August 1997*, Chapter 4, pp. 85–110.

Holtslag, A. A. M.: 2003, 'GABLS Initiates Intercomparison for Stable Boundary Layer Case', *GEWEX News* **13**, 7–8.

Holtslag, A. A. M. and Nieuwstadt, F. T. M.: 1986, 'Scaling the Atmospheric Boundary Layer'. *Boundary-Layer Meteorol.* **36**, 201–209.

Khairoutdinov, M. F. and Randall, D. A.: 2003, 'Cloud Resolving Modeling of the ARM Summer 1997 IOP.: Model Formulation, Results, Uncertainties, and Sensitivities', *J. Atmos. Sci.* **60**, 607–625.

King, J. C., Connolley, W. M., and Derbyshire, S. H.: 2001, 'Sensitivity of Modelled Antarctic Climate to Surface and Boundary-Layer Flux Parametrizations', *Quart. J. Roy. Meteorol. Soc.* **127**, 779–794.

Koren, B.: 1993, 'A Robust Upwind Discretization Method for Advection, Diffusion and Source Terms', *Notes Numer. Fluid Mech.* **45**, 117–138.

Kosovic, B.: 1997, 'Subgrid-scale Modelling for the Large-Eddy Simulation of High-Reynolds-Number Boundary Layers', *J. Fluid Mech.* **336**, 151–182.

Kosovic, B. and Curry, J. A.: 2000, 'A Large Eddy Simulation Study of a Quasi-Steady, Stably Stratified Atmospheric Boundary Layer', *J. Atmos. Sci.* **57**, 1052–1068.

Lewellen, D. C. and Lewellen, W. S.: 1998, 'Large-Eddy Boundary Layer Entrainment', *J. Atmos. Sci.* **55**, 2645–2665.

Lewellen, D. C., Lewellen, W. S., and Xia, J.: 2000, 'The Influence of a Local Swirl Ratio on Tornado Intensification near the Surface', *J. Atmos. Sci.* **57**, 527–544.

Lilly, D. K.: 1967, 'The Representation of Small-Scale Turbulence in Numerical Simulation Experiments', *Proc, IBM Scientific Computing Symp. Environ. Sci,* pp. 195–210.

Louis, J. F.: 1979, 'A Parametric Model of Vertical Eddy Fluxes in the Atmosphere', *Boundary-Layer Meteorol.* **17**, 187–202.

Mahrt, L.: 1987, 'Grid-Averaged Surface Fluxes', *Mon. Wea. Rev.* **115**, 1550–1560.

Mason, P. J.: 1994, 'Large-Eddy Simulation: A Critical Review of the Technique', *Quart. J. Roy. Meteorol. Soc.* **120**, 1–26.

Mason, P. J. and Derbyshire, S. H.: 1990, 'Large-Eddy Simulation of the Stably-Stratified Atmospheric Boundary Layer', *Boundary-Layer Meteorol.* **53**, 117–162.

Moeng, C.-H., Cotton, W., Stevens, B., Bretherton, C., Rand, H., Chlond, A., Khairoutdinov, M., Krueger, S., Lewellen, W., MacVean, M., Pasquier, J., Siebesma, A., and Sykes, R.: 1996, 'Simulation of a Stratocumulus-Topped Planetary Boundary Layer: Intercomparison among Different Numerical Codes', *Bull. Amer. Meteorol. Soc.* **77**, 261–278.

Nieuwstadt, F. T. M.: 1984, 'The Turbulent Structure of the Stable, Nocturnal Boundary Layer', *J. Atmos. Sci.* **41**, 2202–2216.

Nieuwstadt, F. T. M.: 1985, 'A Model for the Stationary, Stable Boundary Layer', in J. C. R. Hunt (ed.), *Turbulence and Diffusion in Stable Environments*, Oxford University Press, pp. 149–179.

Persson, P. O. G., Fairall, C. W., Andreas, E. L., Guest, P. S., and Perovich, D. K.: 2002, 'Measurements Near the Atmospheric Surface Flux Group Tower at SHEBA: Near Surface Conditions and Surface Energy Budget', *J. Geophys. Res.* **107**(C10), 8045, doi:10.1029/ 2000JC000705.

Poulos, G. S., Blumen, W., Fritts, D. C., Lundquist, J. K., Sun, J., Burns, S. P., Nappo, C., Banta, R., Newsom, R., Cuxart, J., Terradellas, E., Balsley, B., and Jensen, M.: 2002, 'CASES-99: A Comprehensive Investigation of the Stable Nocturnal Boundary Layer', *Bull. Amer. Meteorol. Soc.* **83**, 555–581.

Raasch, S. and Etling, D.: 1991, 'Numerical Simulations of Rotating Turbulent Thermal Convection', *Beitr. Phys. Atmos.* **64**, 185–199.

Raasch, S., and Schröter, M.: 2001, 'PALM – A Large-Eddy Simulation Model Performing on Massively Parallel Computers', *Meteorol. Z.* **10**, 363–372.

Saiki, E. M., Moeng, C.-H., and Sullivan, P. P.: 2000, 'Large-Eddy Simulation of the Stably Stratified Planetary Boundary Layer', *Boundary-Layer Meteorol.* **95**, 1–30.

Sullivan, P. P., McWilliams, J. C., and Moeng, C.-H.: 1994, 'A Subgrid-Scale Model for Large-Eddy Simulation of Planetary Boundary-Layer Flows', *Boundary-Layer Meteorol.* **71**, 247–276.

Troen, I. B. and Mahrt, L.: 1986, 'A Simple Model of the Atmospheric Boundary Layers: Sensitivity to Surface Evaporation', *Boundary-Layer Meteorol.* **37**, 129–148.

Van de Wiel, B. J. H., Moene, A. F., Hartogensis, O. K., de Bruin, H. A. R., and Holtslag, A. A. M.: 2003, 'Intermittent Turbulence in the Stable Boundary Layer Over Land. Part III: A Classification for Observations During CASES-99', *J. Atmos. Sci.* **60**, 2509–2522.

Vogelezang, D. H. P. and Holtslag, A. A. M.: 1996, 'Evaluation and Model Impacts of Alternative Boundary-Layer Height Formulations', *Boundary-Layer Meteorol.* **81**, 245–269.